Neutron diffraction determination of the thermodynamic derivatives of the microscopic structure of liquid parahydrogen

M. Zoppi and M. Celli
Consiglio Nazionale delle Ricerche, Istituto di Elettronica Quantistica, Via Panciatichi 56/30, I-50127 Firenze, Italy

A. K. Soper
Rutherford Appleton Laboratory, ISIS Neutron Facility, Chilton, Didcot, OX11 0QX, United Kingdom
(Received 19 March 1998; revised manuscript received 7 May 1998)

We have measured, using time-of-flight neutron diffraction, the thermodynamic derivatives of the microscopic structure factor of liquid parahydrogen in the vicinity of the triple point. Experiments have been carried out on the $T=17.1$ K isotherm and on the $n=22.2$ nm^{-3} isochore so that the thermodynamic derivatives at constant temperature and density could be evaluated. The hydrogen data have been compared with the corresponding quantities for deuterium and quantitatively significant differences have been observed. Assuming that hydrogen and deuterium experience the same intermolecular potential, these differences can only be attributed to the different quantum behaviors of the two molecules. [S0163-1829(98)04938-8]

I. INTRODUCTION

Experimental investigations of the microscopic structure factor of quantum liquids have missed one of the most interesting cases. Following determinations of the structure factor of helium over a wide range of thermodynamic state points[1] and liquid neon,[2] the structure factor of liquid deuterium was measured both in the vicinity of the triple point[3,4] and close to the freezing transition.[5] However, due to the large incoherent neutron scattering cross section of protons, neutron diffraction experiments on light hydrogen have so far, to our knowledge, not been attempted.

There are several reasons to derive experimental information on the microscopic structure of hydrogen. The peculiar behavior of a quantum liquid can be considered to arise from the delocalization of the particles, due to the spread of its wavepacket as measured by the DeBroglie thermal wavelength $\Lambda_{\mathrm{DB}}=h/(2\pi M k_B T)^{1/2}$.[6] Here h is the Planck's constant, k_B is the Boltzmann constant, M is the particle mass, and T is the temperature. When Λ_{DB} becomes sizeable with respect to σ (the hard core diameter of the particle) quantum diffraction effects start to emerge. However, the particles retain their distinguishability and Boltzmann statistics still applies. In contrast, at very low temperature, when Λ_{DB} becomes comparable with the average interparticle distance l, the delocalization is such as to allow the occurrence of exchange effects, and quantum statistics begins to play a role.

The comparison between Λ_{DB}, σ, and l, for the simplest quantum liquids is reported in Table I. It appears that in helium the exchange quantum effects are always important. In particular, when $\Lambda_{\mathrm{DB}}/l=1.66$, the effect becomes macroscopic with the appearance of the superfluid phase. For hydrogen, the overlap of the wavefunctions of two neighboring molecules is much smaller ($\Lambda_{\mathrm{DB}}/l<1$), although the spread of the molecular wave packet exceeds the size of σ at the triple point. In deuterium and in neon the exchange effects are even smaller. The value of Λ_{DB} never exceeds the size of σ and, to reproduce the experimental data, it is sufficient to take into account the quantum diffraction effect only. However, while for liquid deuterium Λ_{DB} is a sizeable fraction of σ, and therefore quantum effects are rather large, in neon Λ_{DB} never exceeds $\sigma/3$ and therefore a reduced influence of quantum behavior is expected. In fact, a fully quantum-mechanical simulation procedure is necessary to reproduce the microscopic structure factor of liquid deuterium,[7] while a much simpler quantum correction procedure is sufficient to obtain the microscopic structure of liquid neon.[8] A similar quantum correction procedure, applied to liquid deuterium, is shown to diverge at small distances.[8]

Thus, it seems that for hydrogen we are facing a situation where quantum diffraction effects are very important but the exchange phenomena are expected to be still limited. Such an intermediate case is very important because theories and simulation techniques are much more easily implemented in absence of quantum exchange, when the individual molecules can be modeled as Boltzmann particles. However, in spite of the importance of hydrogen and the interest in its microscopic structure, there is a lack of experimental information from both neutron and x-ray scattering.

There are two main reasons for the lack of neutron diffraction data. First the ratio, in molecular hydrogen, between the coherent and incoherent scattering cross sections for neutron scattering is very unfavorable. For molecular hydrogen, the incoherent scattering cross section is almost two orders of magnitude larger than the coherent one. In fact the incoherent scattering cross section is still relatively small for low-energy neutrons ($E_0 \leqslant 14.5$ meV),[9] that is, for neutrons which are unable to excite the first rotational transition. However, neutrons of such a low energy are almost useless to determine the microscopic structure factor.

The second reason is related to the role played by inelastic scattering effects. The way the inelastic scattering contributions affect the measured diffraction pattern, and how the experimental data can be corrected for it, have been the subject of much work.[10,11] This correction is obviously more difficult for a molecular system than for a monatomic one,

TABLE I. Evaluation of quantum effects for common quantum liquids. The subscript CP and TP refer to the critical point and to the triple point, respectively. For helium, TP indicates the λ point. Λ_{DB} is the DeBroglie wavelength defined in Sec. I. The parameters σ and l represent the hard core diameter of the particle and the average interparticle distance, respectively.

System	T_{CP} (K)	T_{TP} (K)	n_{CP} (nm^{-3})	n_{TP} (nm^{-3})	$(\Lambda_{DB}/\sigma)_{CP}$	$(\Lambda_{DB}/\sigma)_{TP}$	$(\Lambda_{DB}/l)_{CP}$	$(\Lambda_{DB}/l)_{TP}$
He	5.20	2.18	10.47	21.99	1.50	2.31	0.84	1.66
H_2	33.19	13.96	9.00	23.06	0.72	1.11	0.44	0.94
D_2	38.34	18.71	10.44	25.99	0.47	0.68	0.31	0.60
Ne	44.4	24.55	14.31	37.2	0.21	0.29	0.14	0.26

and at the present time no quantitatively reliable method of subtracting the inelastic scattering from hydrogen containing materials is available. Two features related to the effects of inelastic scattering on the diffraction spectra are of interest here. First, their importance increases with the scattering angle. As a consequence, if for example a neutron diffraction experiment is carried out at a reactor source, where the variation in the exchanged momentum $\hbar Q$ is obtained by changing the scattering angle θ, the inelasticity appears as a typical fall-off of the measured intensity as a function of θ. Secondly, the inelastic scattering effects are larger for light mass systems. Since the critical parameter is the ratio between the mass of the neutron and that of the target particle, the correction procedure first introduced by Placzek,[10] which relies on an expansion in the mass ratio, becomes unmanageable when this ratio is 1/2 (molecular hydrogen). That is the maximum value for any substance. In addition, if the important ratio were that relative to the atomic mass in the molecule, then the mass ratio becomes 1:1 for hydrogen and the Placzek expansion is completely unworkable.

In this case there is an intrinsic advantage in using time-of-flight (TOF) neutron diffraction for measuring the static structure factor $S(Q)$ of liquids composed of light molecules, which is simply related to the fact that here the scattering angle is kept fixed and the spread in Q is obtained from the energy distribution of the incident neutrons. The inelasticity effect is now roughly constant with increasing Q, and nearly zero for low scattering angles, except at low Q where the small mass ratio is once again apparent, and the inelasticity correction rises noticeably above the large Q limit. In principle, the effect could be computed and corrected for. However, the calculation depends again, critically, on the mass ratio between the neutron and the molecule and, in addition, it needs to be computed for a very wide energy distribution of the incident neutrons.

Therefore any correction procedure is not fully reliable, but the availability of pulsed neutron sources, and in particular the possibility of working at small scattering angle, has made it possible to greatly reduce the problem of the inelasticity corrections and to perform accurate diffraction experiments on light fluids: the static structure factor of liquid deuterium has in fact been recently measured to good accuracy[3,5] using this technique.

Thus the residual difficulty for performing an experiment on hydrogen is the unfavorable ratio between the coherent and the incoherent cross section. Because of this ratio, the coherent scattering contribution, which carries the information on the intermolecular structure, is expected to become almost invisible due to the overwhelming incoherent background. In fact, a rough calculation,[12] assuming that the intermolecular (center of mass) structure factor of liquid H_2 is similar to that of D_2, would predict a coherent modulation of the order of 4% of the incoherent background. So, the experiment appears to be intrinsically difficult. However, the situation improves if pure parahydrogen is considered. In fact, in this case, due to the decrease of the intramolecular scattering term at low Q for parahydrogen, this ratio becomes 10% in the region of the first structure factor peak and the experiment appears feasible with a reasonable accuracy.

Based on this premise we have carried out a neutron diffraction experiment on liquid parahydrogen using pulsed neutrons and a low scattering angle diffractometer. In this paper the results we report represent a real breakthrough in the experimental access to the microscopic properties of liquid hydrogen. In Sec. II we give a detailed description of the experimental setup. The description of the analysis of the raw data and the extraction of the useful information is described in Sec. III. Finally, in Sec. IV, we discuss the results.

II. EXPERIMENT DESCRIPTION

The experiment was carried out on the Small Angle Neutron Diffractometer for Amorphous and Liquid Samples (SANDALS) of the pulsed neutron source ISIS (U.K.). A cylindrical sample container (internal diameter 6 mm, external diameter 6.35 mm, height 80 mm), made of vanadium, was fixed to a copper thermal bypass that was designed to stay outside the neutron beam. This, in turn, was connected to the cold finger of a closed circuit helium refrigerator (for a schematic drawing see, for example, Ref. 5). The vanadium container was connected with the external gas handling system by means of a 1/16 in. OD stainless steel tube, wrapped with an electric heater to avoid blockage. Inside the scattering cell, out of the neutron path, we had inserted a solid catalyst made of Cr_2O_3-γAl_2O_3, in order to increase the rate of conversion from orthohydrogen to parahydrogen.

As a first operation, we carried out a background run, at room temperature, with the sample container removed from the beam, but with the cryostat in place. Then, the vanadium container (empty) was placed in the beam and a second run, still at room temperature, was recorded. In this way, we could use the empty container to calibrate the detectors efficiency. The cryostat was then cooled down to 17.0 K and a second empty container run was measured.

Liquid hydrogen was condensed directly into the scatter-

TABLE II. Details on the thermodynamic conditions of the experiment. The estimated error on the temperature is 0.1 K, that on the pressure is 0.1 bar, and that on the density is 0.03 nm^{-3}.

State	T (K)	p (bar)	n (nm^{-3})
1	17.1	2.0	22.22
2	17.1	29.9	23.00
3	20.3	29.9	22.22
4	17.1	16.2	22.61
5	18.6	15.9	22.19

ing cell, stabilized at $T=17.1$ K, keeping an external pressure of ~ 2 bar. The liquid sample was then subjected to small, rapid, temperature variations so that the induced turbulence led to a continuous and efficient interaction with the catalyst. The rate of convergence was measured observing the low-Q behavior of the scattering cross section. In fact, the region $Q \rightarrow 0$ of the diffraction cross section of parahydrogen is much lower (0.56 barn/molecule/sterad) than the corresponding cross section for normal hydrogen (13.28 barn/molecule/sterad).[12] Therefore, we could observe, in real time, the evolution of the sample towards thermodynamic equilibrium. This was reached in a few hours, with an estimated mixture composed of 99.96% of parahydrogen.

Five thermodynamic points were measured in the vicinity of the triple point, in the pressure range between 2 and 30 bar. Three points were selected on the $T=17.1$ K isotherm and three on the $n=22.2$ nm^{-3} isochore. For each thermodynamic point we measured four independent subruns of 500 μAh integrated proton current of ISIS, corresponding to a total measuring time of $\sim 14-16$ h. The details of the experimental conditions are reported in Table II. The densities of the samples have been derived using Ref. 13. The temperature stability of the sample was found very good and within 0.2 K with respect to the set point during the whole experiment. Finally, at the end of the experiment, we carried out a further calibration run, using a vanadium rod in place of the scattering cell, in order to avoid any possible problem in the following analysis.

III. DATA ANALYSIS AND RESULTS

The raw data were collected on 14 detector banks, at various scattering angles, distributed between 3.8° and 31.2°. We used the standard routine package ATLAS (Ref. 14) to correct the raw data for background and container scattering, absorption, and multiple scattering. Each spectrum (one for each different scattering angle) was then converted to the final scattering cross section (per molecule) and was normalized to absolute units using the vanadium empty can as a reference sample. A test calibration procedure, carried out using the vanadium rod sample, gave similar spectra within the experimental errors. In Fig. 1 we show a typical diffraction pattern of liquid parahydrogen. Most of the features observed in the figure are due to the hydrogen intramolecular structure. The large decrease of the measured cross section at low-Q is peculiar to parahydrogen in the state $J=0$. The spectral features that carry the information on the intermolecular structure are hardly visible on this scale and are located in the region of $Q \sim 2$ $Å^{-1}$. In particular, the peak of

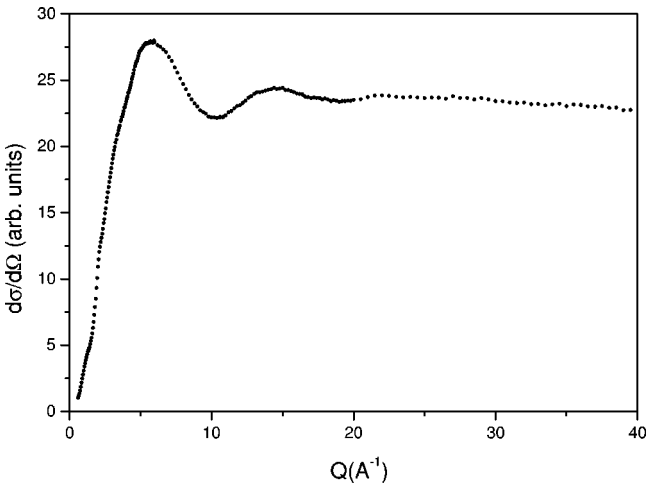

FIG. 1. Raw diffraction pattern of liquid parahydrogen before applying the correction procedures. The main features are of intramolecular origin, while the intermolecular contribution is hardly visible in the region of 2 $Å^{-1}$ (10–12 units on the vertical scale). The falling down of the spectrum at low Q is characteristic of parahydrogen and indicates a full conversion of the sample to the equilibrium composition.

the intermolecular structure factor appears as a tiny shoulder that is located around 10–12 units of the vertical scale of the cross section. Here, we see the advantage of working with parahydrogen. Had we used normal hydrogen, the low-Q region would have been at the same level, or even higher, of the high-Q background. Therefore, the intermolecular structure would have been superimposed on an intramolecular signal 2–3 times larger than in that case.

To extract the intermolecular information from the intramolecular background it is noted that, for a homonuclear diatomic molecule, the measured total cross section can be expressed as[3]

$$\frac{d\sigma}{d\Omega} = u(Q)[S(Q)-1] + v(Q) + P(Q), \tag{1}$$

where $S(Q)$ is the static structure factor of the molecular centers of mass and the functions $u(Q)$ and $v(Q)=v(Q,t=0)$ are molecular form factors which are interpreted as the *intermolecular* and *intramolecular* neutron cross sections, respectively. The unknown function $P(Q)$ accounts for the inelastic scattering corrections. We point out that writing Eq. (1) implies neglecting completely the orientational correlations. This is a reasonable assumption for liquid hydrogen, as it is well known that the same assumption is well verified even in the solid phase.[15]

If a free rigid-rotor model is applied, then the expressions for the molecular form factors assume a very simple analytical form.[16] However, based on our previous experience with deuterium, we know that this simple model is insufficient and should be generalized. To first order approximation the molecule can be modeled as a freely rotating harmonic oscillator. In this case, the molecular form factors are also known and can be expressed as a sequence of functions approximating the true behavior.[12] To the lowest order, the

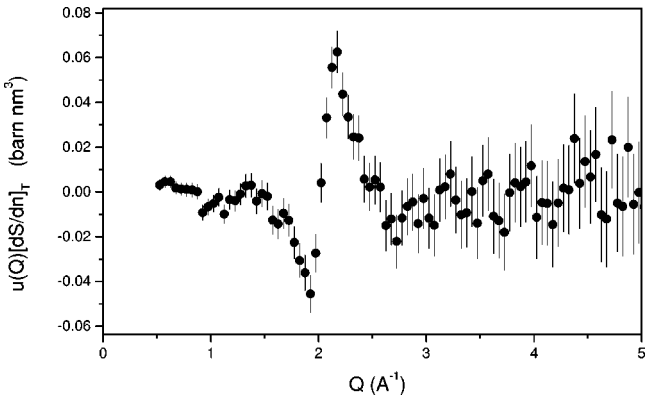

FIG. 2. Average (over the 14 detector banks) of the difference spectrum at constant temperature ($T=17.1$ K) and different densities ($n=23.0$ and 22.2 nm^{-3}). The noisy regions come out averaged to zero (within the errors) while a rather nice picture emerges in the region of 1.5–3.0 Å^{-1}.

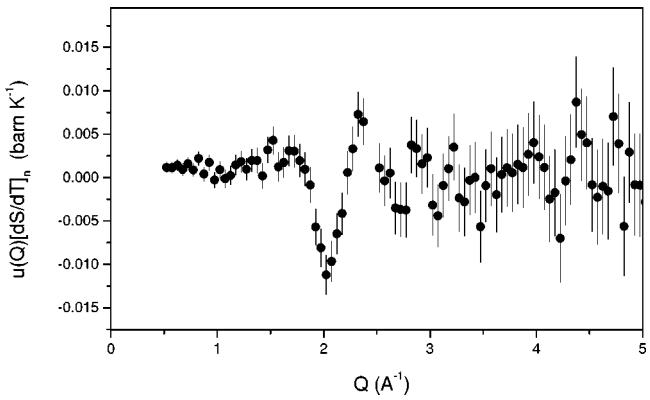

FIG. 3. Average (over the 14 detector banks) of the difference spectrum at constant density ($n=22.2$ nm^{-3}) and different temperatures ($T=20.3$ and 17.1 K). The noisy region is mainly at high Q and is averaged to zero (within the errors). A rather clear behavior emerges in the region of 1–3 Å^{-1}.

functions $u(Q)$ and $v(Q)$ are the familiar rigid rotor functions that are now modulated by a Debye-Waller factor. For pure parahydrogen, these are

$$u^{(0)}(Q)=4a_{\mathrm{coh}}^2\left[\exp\left(-\frac{\lambda_{\mathrm{DW}}^2Q^2}{2}\right)\frac{\sin(QD_e/2)}{(QD_e/2)}\right]^2 \qquad (2)$$

and

$$v^{(0)}(Q)=2(a_{\mathrm{coh}}^2+a_{\mathrm{inc}}^2)+2(a_{\mathrm{coh}}^2-a_{\mathrm{inc}}^2)\times\exp(-2\lambda_{\mathrm{DW}}^2Q^2)\frac{\sin(QD_e)}{(QD_e)}, \qquad (3)$$

where $\lambda_{\mathrm{DW}}=(\hbar/2M\omega_v)^{1/2}=0.0044829$ nm is the Debye-Waller wavelength, M is the molecular mass, and ω_v is the circular frequency of the molecular vibration. The parameter D_e represents the average equilibrium distance of the two nuclei ($D_e=0.074144$ nm). The scattering lengths are $a_{\mathrm{coh}}=-3.741$ fm and $a_{\mathrm{inc}}=25.28$ fm.[17] The sequences converge rapidly and it is found that their limiting behavior can be well represented by Eqs. (2) and (3) if the parameters λ_{DW} and D_e are substituted with slightly different effective parameters.[12] The effective values used here were $\lambda_{\mathrm{DW}}=0.004\,517\,4$ nm and $D_e=0.073032$ nm.

A similar procedure was successfully used to analyze the diffraction data of deuterium.[3,5] In the present case, however, the same procedure could not be applied to the present hydrogen data. In fact, the size of the inelastic scattering corrections, that is expected to be proportional to the total cross section, becomes now relevant. In other words, the correction term $P(Q)$, that was neglected in the deuterium experiments owing to the small scattering angle configuration, now seems to play a relevant role and should be taken explicitly into account. In addition, due to the magnitude of the intramolecular contribution to the scattering cross section, even small fluctuations in the instrument electronics become now crucial and tend to generate noise that submerges the signal. For these reasons, we decided to use a different procedure that was already successfully tested in the analysis of the diffraction spectra from water and therefore should solve, in principle, the same class of problems.[18]

The procedure adopted was to fit a Chebyshev polynomial of a suitable low order to the data. The order was chosen high enough to remove as much as possible any divergence of the scattering at low Q, but sufficiently low that it did not remove any of the important intermolecular interference structure at larger Q. The difference between the data and this polynomial was then subject to a Fourier transform, and any structure at unphysically low r values was back transformed to Q space to yield a correction to the polynomial background. Finally the full background, polynomial plus Fourier transform, was subtracted from the diffraction data to yield the interference differential scattering cross section. The degree to which this incoherent background subtraction procedure is effective was assessed by comparing the interference functions obtained from different scattering angle banks of detectors. Good overlap between the banks after subtraction indicated that the procedure had been successful.

The analysis was then completed, taking advantage of the same standard routines that were used in the case of liquid water,[18] to subtract the intramolecular portion from the diffraction spectrum. The resulting intermolecular contribution, however, still turns out to have too large systematic errors to enable a realistic comparison with the available theories. However, when we attempted to evaluate the thermodynamic derivatives of the structure factor, we were pleased to find a better agreement among the various spectra. In fact, a raw superposition of the 14 difference spectra taken at constant temperature ($T=17.1$ K) and different densities (23.0 and 22.2 nm^{-3}) reveals that the region around 2 Å^{-1} carries a definitely clear information out of a generalized noise. The same is true for the 14 difference spectra taken at constant density (22.2 nm^{-3}) and different temperatures (20.3 and 17.1 K). Basing on these results, we have averaged the 14 difference spectra, taken at constant temperature, obtaining the average density-difference that is reported in Fig. 2. In Fig. 3 we report a similar result for the temperature difference at constant density. The resulting error bars are fairly large, but the behavior of the two functions appear clear and qualitatively similar to that of the corresponding quantities for deuterium (cf. Fig. 6 of Ref. 3).

The evaluation of the thermodynamic derivatives was car-

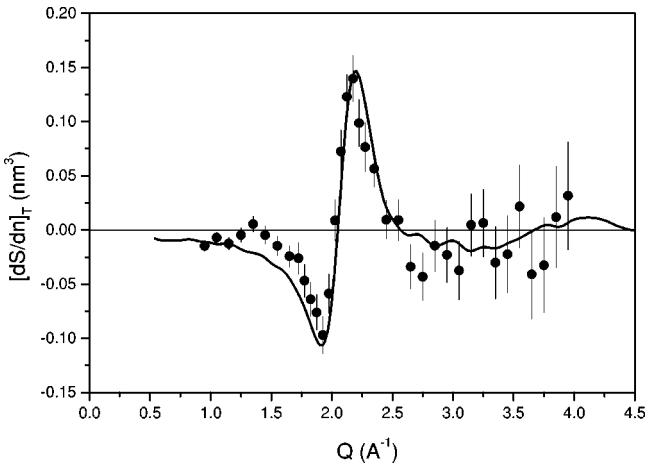

FIG. 4. Experimental determination of the density derivative, at constant temperature, of the intermolecular structure factor $S(Q)$ (black dots with error bars) for liquid parahydrogen at $T=17.1$ K and $n=22.61$ nm^{-3}. The line is a spline fitting to the data of liquid deuterium (cf. Ref. 7) in similar thermodynamic conditions.

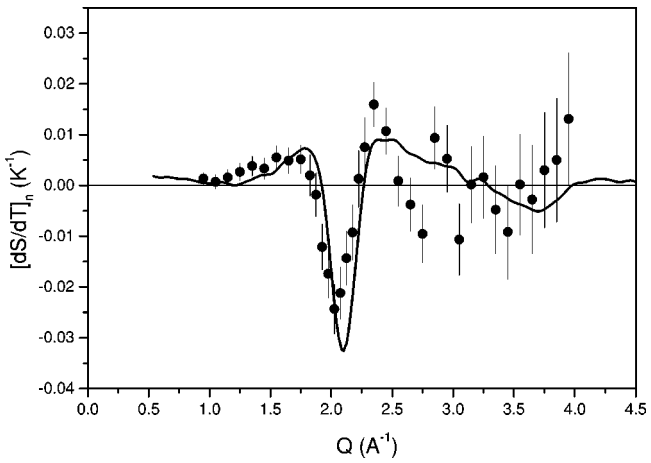

FIG. 5. Experimental determination of the temperature derivative, at constant density, of the intermolecular structure factor $S(Q)$ (black dots with error bars) for liquid parahydrogen at $T=18.7$ K and $n=22.22$ nm^{-3}. The line is a spline fitting to the data of liquid deuterium (cf. Ref. 7) in similar thermodynamic conditions.

ried out in the two points characterized by the pair of thermodynamic coordinates $(n,T)=(22.2$ nm^{-3}, 18.6 K) and (22.6 nm^{-3}, 17.1 K). Since the spectra were measured in five thermodynamic points (cf. Table II), we could estimate both the left and right thermodynamic derivatives for two thermodynamic points. These were found in good agreement, within the respective experimental errors. Making use of the experimental differences, and of Eq. (1) to remove the molecular form factor, we were able to obtain the average of $[\partial S(Q)/\partial n]_T$, for the first case. In the second case, we have obtained the average of $[\partial S(Q)/\partial T]_n$. The measured thermodynamic derivatives of $S(Q)$ are reported in Figs. 4 and 5. In both cases we observe that the error bars increase, by increasing the momentum transfer, and that the data are significant only up to ~ 4 Å^{-1}. However, based on the behavior of the corresponding quantities for deuterium, we may safely assume that the thermodynamic derivatives vanish beyond this point. The full lines that are reported in the same figures represent the density and temperature derivatives, respectively, of the $S(Q)$ of liquid deuterium, measured in similar thermodynamic conditions (the reason behind the choice of a continuous line is that the experimental errors on the deuterium data are much smaller than the present errors on parahydrogen).

IV. DISCUSSION

By means of time-of-flight neutron diffraction, we have measured the thermodynamic derivatives of the structure factor of liquid parahydrogen close to the triple point. Due to the large incoherent background the experimental determination of $S(Q)$ appears noisy and of a limited practical utility. The density derivative, at constant temperature, is reported in Fig. 4 for the thermodynamic point $n=22.6$ nm^{-3} and $T=17.1$ K. In Fig. 5 we have reported the temperature derivative, at constant density, for the thermodynamic point $n=22.2$ nm^{-3} and $T=18.6$ K.

Starting from the low-Q side, it is interesting to observe that, in Fig. 4, the negative peak appears sharper, while the rising edge, and the whole positive peak, are shifted to lower Q values than in the case of deuterium. The latter feature is also apparent in the temperature derivative of Fig. 5. While for the first observation we are not able to give a simple, intuitive, explanation, the second is consistent with the expected increase of the quantum effects in hydrogen. In fact, when the data are plotted in reduced units of Q (i.e., as a function of $Q^*=Q\sigma$, where σ is the effective molecular diameter), it can be noted that the rising edge and the positive peak of the density derivative, and the whole temperature derivative, become almost coincident, for the two cases, provided that the effective diameter of hydrogen is increased by $\sim 2\%$.

With respect to deuterium, liquid hydrogen is expected to show larger quantum effects. One aspect of the increased quantum behavior is the observed increment in the effective molecular size of hydrogen with respect to deuterium. If we reasonably assume that the two isotopes experience the same intermolecular potential, since that is determined by the same electronic structure, we note that the observed increase of the effective molecular size is a signature of the expanded single particle wave function.

It would be interesting to compare the present experimental results with a calculation for the same systems. A suitable technique is presently available and uses a quantum-mechanical computer simulation based on the path integral Monte Carlo method. However, this task exceeds the aims of the present work.

[1] H.R. Glyde and E.C. Svensson, in *Methods of Experimental Physics*, edited by D.L. Price and K. Sköld (Academic, London, 1987), Vol. 23 B, Chap. 13 and references therein.
[2] L.A. de Graaf and B. Mozer, J. Chem. Phys. **35**, 4697 (1971); M.C. Bellissent-Funel, U. Buontempo, A. Filabozzi, C. Petrillo, and F.P. Ricci, Phys. Rev. B **45**, 4605 (1992).
[3] M. Zoppi, U. Bafile, R. Magli, and A.K. Soper, Phys. Rev. E **48**, 1000 (1993).
[4] E. Guarini, F. Barocchi, R. Magli, U. Bafile, and M.C. Bellissent-Funel, J. Phys.: Condens. Matter **7**, 5777 (1995).
[5] M. Zoppi, A.K. Soper, R. Magli, F. Barocchi, U. Bafile, and N.W. Ashcroft, Phys. Rev. E **54**, 2773 (1996).
[6] U. Balucani and M. Zoppi, *Dynamics of the Liquid State* (Oxford University Press, Oxford, 1994).
[7] M. Zoppi, U. Bafile, E. Guarini, F. Barocchi, R. Magli, and M. Neumann, Phys. Rev. Lett. **75**, 1779 (1995).
[8] F. Barocchi, M. Neumann, and M. Zoppi, Phys. Rev. A **31**, 4015 (1985).
[9] J.A. Young and J.U. Koppel, Phys. Rev. **135**, A603 (1964).
[10] G. Placzek, Phys. Rev. **86**, 377 (1952).
[11] J.G. Powles, Mol. Phys. **36**, 1161 (1978); **36**, 1181 (1978).
[12] M. Zoppi, Physica B **183**, 235 (1993).
[13] H.M Roder, G.E. Childs, R.D. McCarty, and P.E. Angerhofer (unpublished).
[14] A.K. Soper, W.S. Howells, and A.C. Hannon (unpublished).
[15] J. Van Kranendonk, *Solid Hydrogen* (Plenum, New York, 1983).
[16] V.F. Sears, Can. J. Phys. **44**, 1279 (1966).
[17] S.F. Mughabghab, M. Divadeenam, and N.E. Holden, *Neutron Cross Sections* (Academic, New York, 1981).
[18] A. K. Soper and A. Luzar, J. Chem. Phys. **97**, 1320 (1992).